Progress In Electromagnetics Research C, Vol. 135, 107–119, 2023

Novel Folded Antenna Design and SAR Analysis for WCE and Biomedical Applications

Asmae Mimouni[3, *], Brahim Fady[1], Jaouad Terhzaz[2], Abdelwahed Tribak[1], and Hanan Akhdar[3]

Abstract—This study presents a pioneering curved antenna design that is seamlessly integrated into Wireless Capsule Endoscopy (WCE) devices. The proposed antenna features a miniature height of 25 mm, a radius of curvature of only 5.5 mm, and a conductive line width of up to 2 mm, making it an ideal fit for the use in compact WCE applications. The antenna is specifically designed to operate in the ISM5800 band and achieves outstanding performance metrics, such as an S_{11} of -10 dB and a gain of 5.8 dBi. To evaluate the safety of our design for human usage, we conducted an investigation of the specific absorption rate (SAR) of the Hugo Model antenna in various positions for ISM5800 and compared our findings to the safety limits specified by the Federal Communications Commission (FCC) standards. Our results confirm that the proposed antenna design meets the safety requirements for wireless communication systems in biomedical applications, thereby demonstrating its potential for clinical use.

1. INTRODUCTION

Wireless Capsule Endoscopy (WCE) has evolved to become a promising technology that allows for noninvasive examination of the gastrointestinal (GI) tract. In recent years, WCEs have been designed to incorporate remotely controlled micro-robots with mechanical legs that can stick to specific locations in the GI tract [1]. However, communication with the WCE remains a significant challenge due to the harsh loss medium presented by the heterogeneous dielectric media with irregularly shaped boundaries in the human body [2]. The electrical characteristics (permittivity, permeability, etc.) of each element of the GI, such as the stomach, small intestine, and large intestine, pose different challenges for WCE communication [3]. The main problem for WCE is to improve the image quality and to locate in real-time the capsule inside the human body [4]. This requires optimized antennas inside and on the body at an adequate medical frequency to allow high-speed transmission, and realistic path loss models to calculate the link budget.

Numerous articles have been published on wireless capsule endoscopy technology. Some research attempts to strengthen the advantages of current WCEs, such as reducing the size of the capsule, calculating and improving the propagation and efficiency of transmitting and receiving antennas. Others strive to minimize the drawbacks of capsule endoscopy such as the antenna, printed circuit board (PCB), and battery [5, 6]. In a WCE system, a capsule antenna is the key component, and many efforts have been made in recent years. As the space of the capsule is limited, antenna miniaturization is crucial. Spiral antennas [7, 8] and meander dipole antennas [9] are the common antenna types in capsule antenna designs. Conformal antennas like antennas wrapped [10, 11] or printed on the outer wall [12] of the

Received 31 March 2023, Accepted 8 July 2023, Scheduled 27 July 2023

* Corresponding author: Asmae Mimouni (amalmimouni@imamu.edu.sa).

[1] Department of Microwave and Communication Antenna Subsystems, INPT, Rabat, Morocco. [2] Department of Physics, CRMEF Casablanca-Settat, Casablanca, Morocco. [3] Department of Physics, College of Science, Imam Mohammad Ibn Saud Islamic University (IMSIU), P.O. Box 90950, Riyadh 11623, Saudi Arabia.

capsule are mainly aimed at saving the inner space for other components. Moreover, the capsule travels in the complex body environment characterized by various permittivity values, and a wide bandwidth is typically required. A spiral antenna with a fat arm was proposed to achieve a wide bandwidth [13]. An ultra-wideband (UWB) antenna operating at a 4 GHz center frequency was also analyzed in [14]. However, some proposed antennas lack in certain aspects, such as polarization matching, which can deteriorate communication efficiency [15].

Our research aims to propose a miniaturized antenna that meets the requirements and prerequisites of WCE communication from inside the human body to the final server responsible for processing the captured data. The proposed antenna is a ribbon folded into the capsule next to the side surface to gain space, which is very tight inside the WCE. The proposed antenna transmits the images captured during the journey from the capsule to a second antenna attached to the patient's stomach, which serves as a relay for transmitting data to the final treatment server.

In this paper, we detail the structure of the new cylindrical ribbon antenna integrated and simulated with the realistic human body model HUGO for each tissue of the gastrointestinal system from the throat to the intestines. This antenna being inside the human body must transmit the images with one of the ISM medical frequency bands to guarantee the safety of the patient. The antenna was fabricated and verified using CST Studio Software. Finally, a detailed study of the impact and SAR results has been introduced, providing the proof of compliance of the proposed antenna to FCC standards.

2. SPECIFICATIONS

2.1. Design of a Cylindrical Micro Antenna Optimizing the Space of the Endoscopy Capsule

2.1.1. Configuration of WCE within the Human Body

In realizing a reliable WCE system, the on-board antenna requires working effectively in close proximity to the human body. For such applications, efficient wireless performance is essential. With the added challenges of implementing multiple antennas in an ultra-compact form, it is absolutely essential to consider a wireless solution first. These intimate devices pose a number of design challenges, especially when it comes to wireless transmission. First of all, the antenna should not contain any active component to reduce power consumption. The antenna should be miniaturized as much as possible to fit inside the WCE device having standard dimensions of $26 \times 11\,\text{mm}^2$ [15].

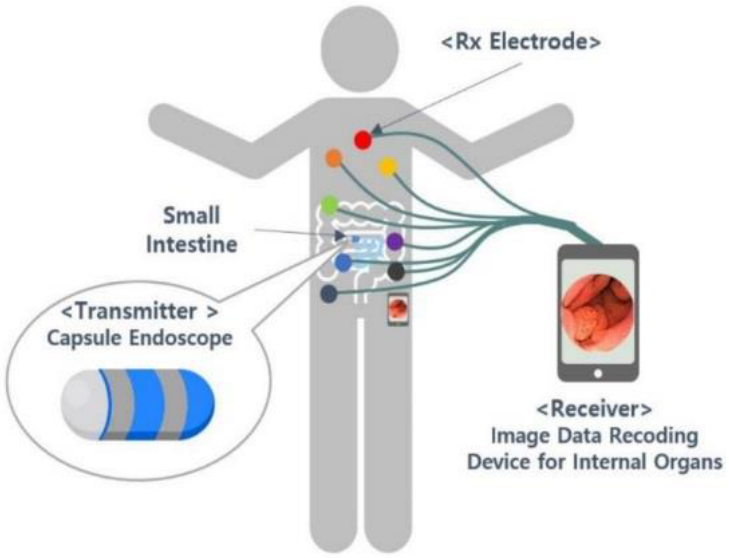

Figure 1. The configuration diagram of the WCE capsule.

The WCE can communicate with external devices such as sensors, wireless headsets, or a heads-up display. Like other computers, a WCE can collect information from internal or external sensors and monitor or retrieve data from other instruments or computers.

Figure 1 illustrates the path of the WCE through the gastrointestinal tract, where it undergoes random movement and spinning, posing challenges for localization. The journey begins in the esophagus, a hollow tube connecting the throat to the stomach. Upon leaving the stomach, the capsule enters the small intestine, which has proven to be the site of significant clinical impact for WCEs. The small intestine, characterized by a curved and coiled tubular structure, spans approximately 6 meters in length (the longest segment of the gastrointestinal tract) and has a diameter of 3 to 4 cm. These intricate curves and coils impede the movement of the WCE, making capsule localization a formidable task. Ultimately, the capsule reaches its destination in the large intestine, also known as the colon, which is typically the area of interest in cases involving colon tumors.

2.1.2. HUGO Voxel-Based Model

In this study, our focus is on the design and performance of the antenna integrated into the WCE. However, it is important to consider the human body model used for simulation purposes, as it impacts the evaluation of the antenna's performance within realistic scenarios.

To accurately represent the environment in which the antenna operates, we utilize a Voxels-based human body model called HUGO [15], as shown in Figure 2. This model provides a foundation for assessing electromagnetic fields and SAR values within the human body. While the primary objective is antenna evaluation, the choice of an appropriate human body model is essential for conducting comprehensive analyses. By incorporating an accurate representation of the human body, including its postural variations, our antenna research can provide insights into the antenna's performance in practical situations. We aim to ensure that the proposed antenna design is evaluated within a realistic context, taking into account the challenges posed by the human body's anatomy and postures during WCE procedures.

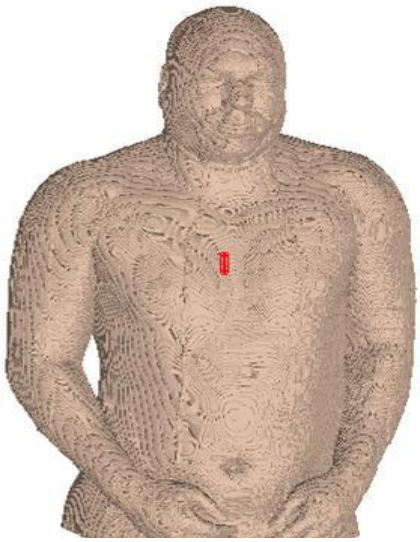

Figure 2. Hugo model supplied by CST.

2.1.3. Parametric Study of the WCE Antenna

We started with a standard planar antenna to get a design. We used the Bending technique to design a structure that provides the ISM 5800 band using the correlation between frequency and wavelength. Then we design the fonts step by step also according to the wavelength and taking into account that each new pipe must not interfere in terms of frequency band with the neighboring arm and must adapt to

the specifications of antenna sizing. At each design stage, we observe and study the current distribution in each frequency in order to adjust and optimize the structure.

Figure 3 illustrates the fundamental steps involved in the design process of our curving planar antenna, specifically tailored to fit within the WCE capsule. Each component of the antenna is meticulously designed to ensure compatibility with the desired frequency band. Throughout the design process, we conducted numerous simulations and iterations to optimize the return loss performance and achieve the desired resonance characteristics. To enable the integration of the antenna within the compact dimensions of the WCE capsule, careful consideration was given to adjusting the sizes and dimensions of the antenna elements. We scaled down the components while ensuring that their geometric configurations align with the capsule's limited space. This precise adjustment allows for seamless integration and optimal utilization of the available area within the WCE capsule.

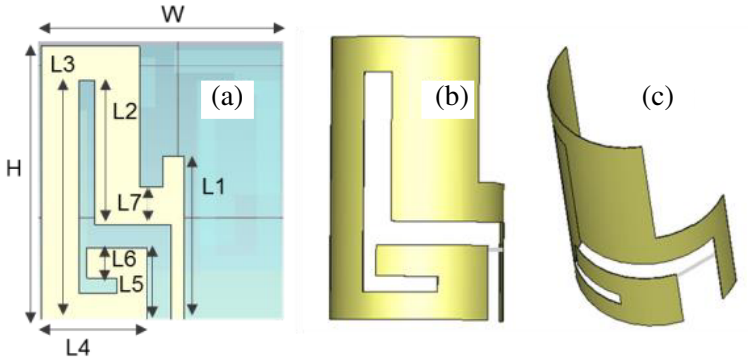

Figure 3. Antenna design steps: (a) initial structure, (b) resizing, (c) bending.

Figure 4 illustrates the S_{11} results of three different configurations corresponding to the steps involved in the antenna design process. Each configuration represents a specific stage: (a) initial structure, (b) resizing, and (c) bending. In the first configuration (conf 1), the planar structure of the antenna demonstrates frequency coverage at 5.5 GHz. This initial design serves as a starting point for further refinement. The second configuration (conf 2) involves resizing the antenna dimensions. This adjustment leads to a shift in the resonance frequency towards higher frequencies, specifically by 0.1 GHz. This step aims to optimize the antenna's performance and align it closer to the desired target frequency band.

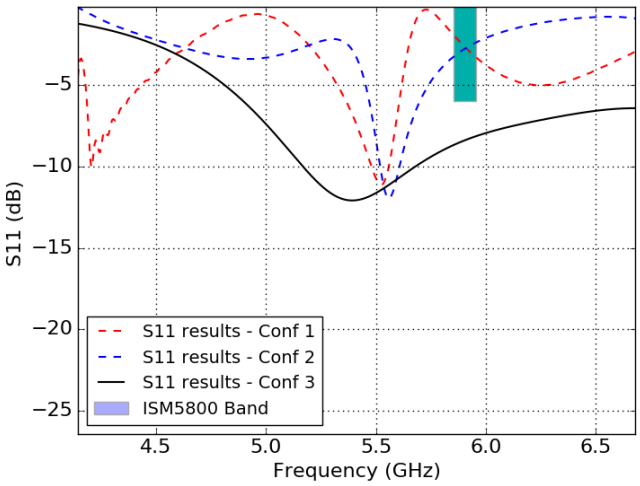

Figure 4. Result of simulation S_{11} of the WCE antenna.

Finally, in the third configuration (conf 3), the structure of the antenna is bent according to the final design specifications. This bending process represents the last step (C) in the antenna design. As a result, the resonance frequency aligns precisely with the target band at 5.8 GHz.

We used for all the simulations the 3D finite difference method of the time domain (FDTD) as implemented in the platform software of CST Studio. The simulations results given in Figure 4 show that the antenna covers the target ISM-5800 band with a reflection coefficient up to −14 dB and bandwidth up to 1500 MHz. The same figure compares the bended structure with the planar structure, and we notice that bending the structure shifted the resonance frequency from 5.4 GHz to the target frequency 5.8 GHz and enhanced the S_{11} with −3 dB.

Table 1 provides a comprehensive summary of the dimensions and key parameters of the proposed antenna design. These specifications play a crucial role in defining the antenna's performance and its compatibility with the WCE system. The table below presents a condensed overview of the design's essential characteristics.

Table 1. Proposed design parameter values.

Parameter	Value
H	22 mm
W	18 mm
$L1$	13 mm
$L2$	11 mm
$L3$	18 mm
$L4$	8 mm
$L5$	6 mm
$L6$	3 mm
$L7$	4 mm

The proposed WCE antenna, shown in Figure 5, has a height of 25 mm, and the radius of curvature is 5.5 mm with the width of the conductive line equal to 2 mm. We used a ribbon substrate with a permittivity tending to 1 and a dielectric tangent loss up to 0.02. The weld spaces are modeled as perfect electric conductor (PEC) surfaces of dimension $2 \times 4\,\text{mm}^2$. We observe that the antenna fits perfectly to the standard dimensions of the WCE.

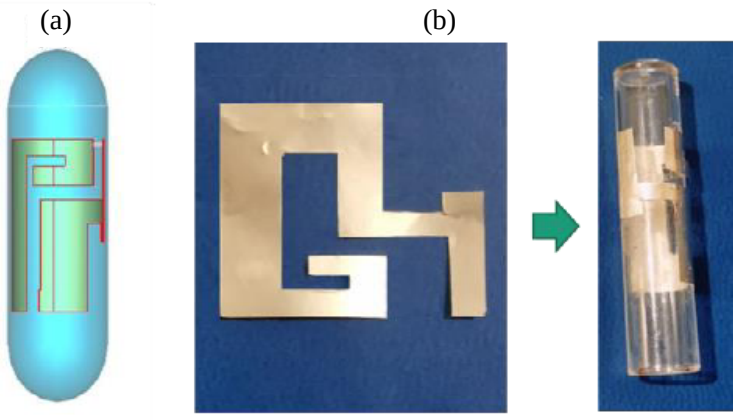

Figure 5. Antenna design: (a) Simulation design, (b) manufactured antenna.

3. MEASUREMENTS AND DISCUSSION

3.1. Reflection Coefficient Results

Figure 6 presents the measurements of the S_{11} parameter conducted in a free space environment. These measurements were performed without the presence of a human body. The focus was to evaluate the antenna's performance in an isolated setting, allowing for an assessment of its impedance matching and frequency band coverage.

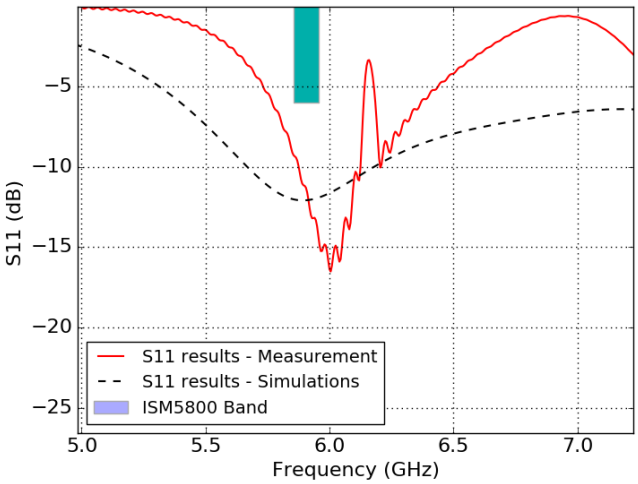

Figure 6. Measurement of S_{11} for the proposed antenna.

The results obtained from the measurements in free space confirm the simulation findings. The S_{11} values recorded demonstrate a maximum of −15 dB, indicating a good impedance match. This suggests that the antenna efficiently transfers power from the transmission line to free space.

Furthermore, the measurements reveal a full coverage of the ISM5800 band, indicating that the antenna is well-suited for wireless communication within this frequency range.

3.2. Radiation Results

Figure 7 presents the 2D gain radiation patterns of the antenna at different frequencies, specifically in azimuthal views at Phi = 0 and Phi = 90. Figure 8 complements the analysis by showcasing the radiation patterns in elevation views.

Analyzing the results depicted in Figure 7 and Figure 8, it becomes evident that the antenna design exhibits an approximately omnidirectional radiation pattern. This characteristic indicates that the antenna radiates or receives signals with relatively uniform strength in various directions around its axis.

Furthermore, the gain of the antenna varies across different frequencies. Notably, at 5800 MHz, the antenna demonstrates the highest gain, reaching up to 3.6 dBi. This signifies that the antenna design offers increased power concentration in a particular direction compared to an isotropic radiator (which has a gain of 0 dBi).

The observed omnidirectional radiation pattern combined with the higher gain at 5800 MHz suggests that the antenna is well-suited for applications requiring broad coverage and enhanced performance in the specified frequency range.

Figure 9 shows the variation of the maximum gain measured in dBi as a function of the frequency. Note that the minimum gain is 3 dBi obtained at 5 GHz, and the maximum gain is 3.6 dBi at 5.8 GHz. We find that the antenna has a high maximum gain over all frequency bands and has a desirable value for the 5800 MHz target band.

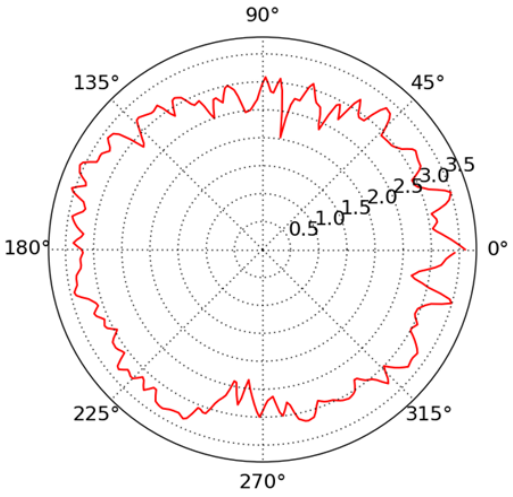

Figure 7. Elevation of the results of the radiation pattern measurements for 5800 MHz.

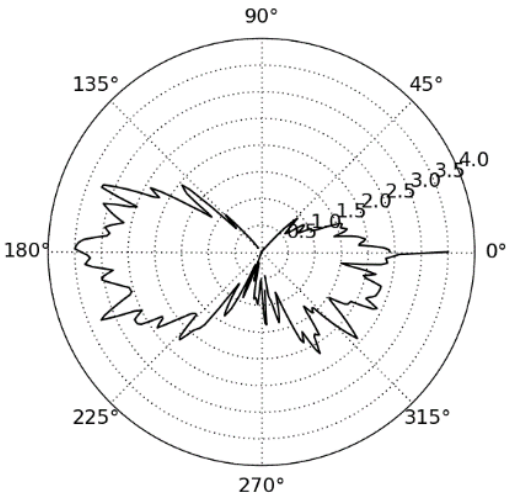

Figure 8. Azimuth of the results of the radiation pattern measurements for 5800 MHz.

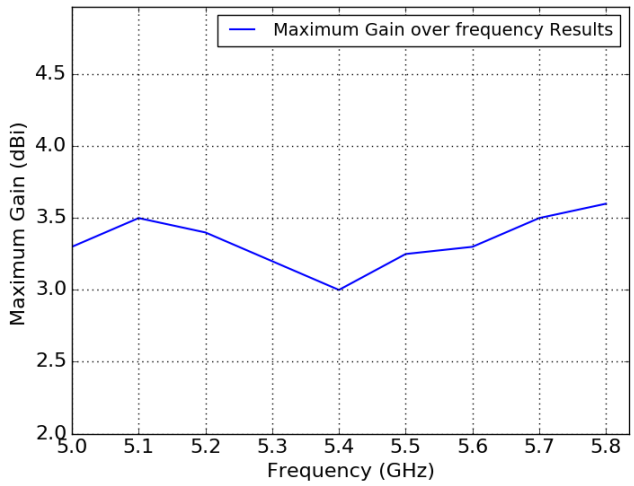

Figure 9. Variation of gain as a function of frequency.

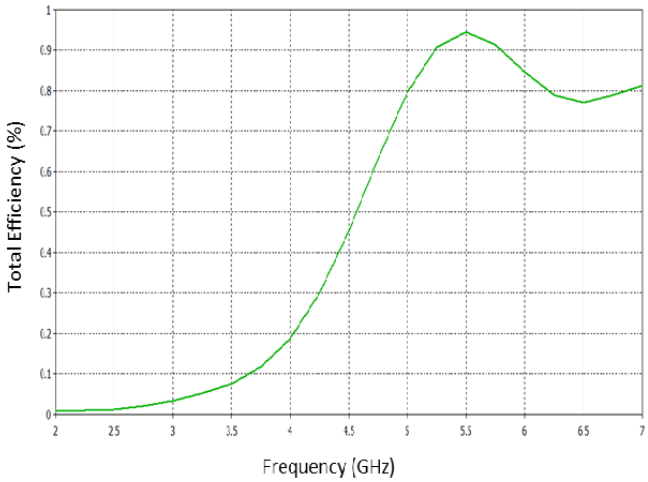

Figure 10. Variation of the total efficiency on the frequencies.

Figure 10 illustrates the total efficiency of the proposed antenna design across the frequency range. Notably, for the targeted band of 5750–5850 MHz, which includes the 5800 MHz frequency, the antenna demonstrates a total efficiency ranging from 85% to 90%. It is important to highlight that the antenna design does not radiate in lower frequencies that fall outside the scope of the study.

The results emphasize that the antenna's highest performance is achieved within the target band, particularly in the ISM5800 and WMAX5200 frequency ranges. In these specific bands, the antenna exhibits an impressive total efficiency of 90%. This efficiency measurement indicates the effectiveness of the antenna in converting input power into radiated electromagnetic energy within the desired frequency range.

The findings emphasize the antenna's suitability and strong performance within the designated target bands, while also highlighting its non-radiation characteristics in frequencies outside the scope of the study.

3.3. Influence of the HUGO Model on the Antenna

After evaluating the reflection and radiation measurements of the antenna in free space, the impact of the human body presented by the HUGO model on the performance of the antenna in terms of S_{11} is studied as per the configuration given in Figure 11.

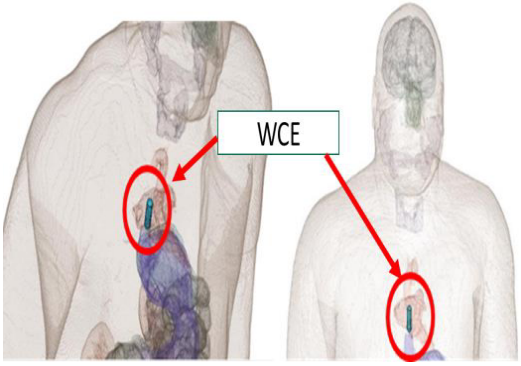

Figure 11. Configuration of the impact simulation of the HUGO model.

Figure 12 shows the influence of the WCE cover on the antenna parameter S_{11}. The S_{11} results of the antenna inside the WCE are compared to the S_{11} results of the free space antenna.

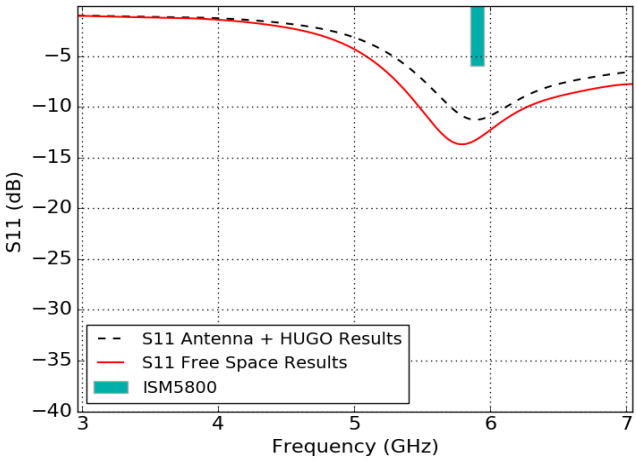

Figure 12. Influence of the HUGO model on the WCE antenna.

To investigate the impact of stomach acid on antenna performance, we conducted additional simulations using the HUGO Model. Specifically, we focused on the behavior of the antenna when it was placed within an acid liquid environment resembling the stomach. As show in Figure 13, the acid was modeled as a cylinder measuring $5 \times 10\,\text{cm}^2$ with gastric acid dielectric properties [21], and the antenna, along with the capsule, was positioned inside this simulated acid environment.

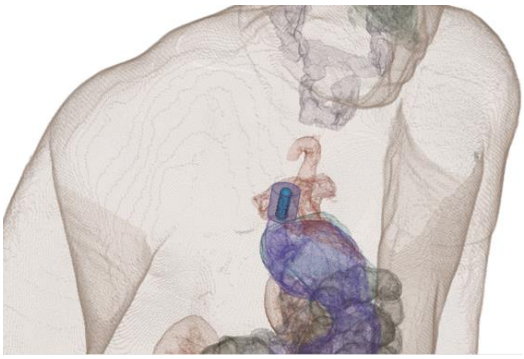

Figure 13. Configuration of antenna inside acid liquid.

The results presented in Figure 14 show that the presence of the acid liquid caused a minor shift in the S_{11} response towards lower frequencies, accompanied by a 2 dBi increase in antenna S_{11}. However, despite these changes, the antenna remained capable of covering the target frequency band ISM5800.

These findings suggest that while the impedance of the antenna is slightly affected by the presence of stomach acid, the performance remains within an acceptable range for our intended application.

3.4. SAR Studies

In this section, we evaluate the SAR performance of the antenna in the intestines of the human body presented by the HUGO model. The SAR values are examined according to the standard limits defined by the FCC standards, i.e., 4 W/kg averaged over 10 g of stomach and intestinal tissue [16]. Figure 15 shows the position of the antenna in the HUGO Gastrointestinal model for the SAR simulation with the CST studio software.

Specific Absorption Rate (SAR) is a measure used to quantify the rate at which electromagnetic energy is absorbed by biological tissues. It is defined as the power absorbed per unit mass of tissue

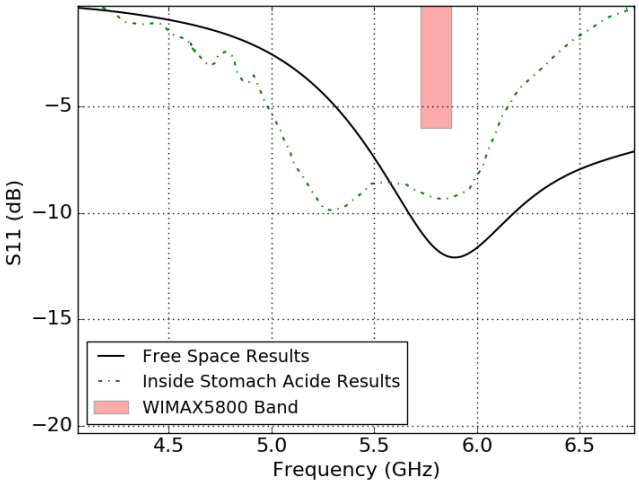

Figure 14. Configuration of antenna inside acid liquid.

Figure 15. Position of the WCE antenna for SAR analysis.

and is typically expressed in watts per kilogram (W/kg). The SAR value can be calculated using the formula [17]:

$$\text{SAR} = (\sigma \times |E|^2)/(\rho \times \rho_0)$$

where σ is the tissue conductivity, $|E|$ the electric field strength, ρ the tissue density, and ρ_0 the reference density.

SAR serves as an important parameter in evaluating the potential health effects of electromagnetic radiation on the human body. Regulatory bodies establish SAR limits to ensure the safe use of wireless communication devices. By assessing SAR values, researchers can better understand the absorption of electromagnetic energy by tissues and develop guidelines to protect public health.

Table 2 provides a comprehensive summary of the dielectric properties and conductivity characteristics of different tissues at each frequency. It highlights the variations in these properties for each tissue type, enabling a better understanding of the electromagnetic behavior within the human body.

Figure 16 presents the three-dimensional distributions of SAR, measured in watts per kilogram (W/kg). The SAR values are averaged over a 10 g mass that was simulated inside the HUGO model specifically for the 5800 MHz frequency. The simulations were conducted using the CST MWS software.

Table 2. Dielectric parameters of HUGO fabrics [16–18].

Tissue type	Relative permittivity	Relative permeability	Conductivity
Skin	41.405334	1	0.86678
Fat	11.333888	1	0.109162
Muscle	56.879063	1	0.995364
Cartilage	42.653103	1	0.782333
Cerebrospinal fluid	68.638336	1	2.412575
Sclera	55.27013	1	1.166726
Vitreous	68.90184	1	1.636162
Lens nucleus	35.841595	1	0.484917
Grey matter	52.724701	1	0.942193
White matter	38.886288	1	0.590815
Nerve	32.530067	1	0.573612
Thyroid	59.683323	1	1.038448
Tongue	55.27013	1	0.936192
Bone	20.787804	1	0.339975
Blood	61.360718	1	1.538069
Air	1	1	0

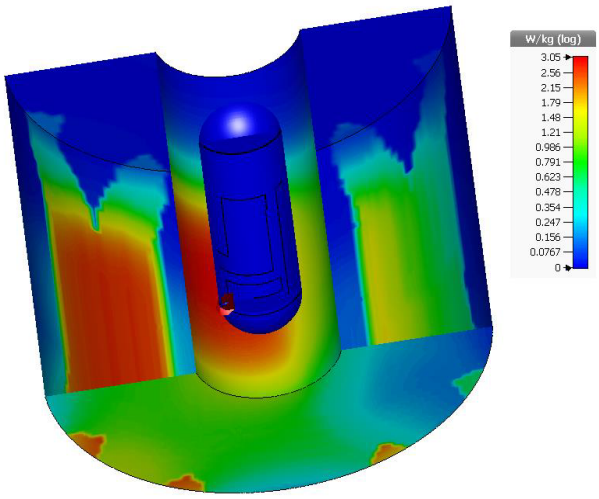

Figure 16. Distribution of SAR averaged over 10 g inside the gastrointestinal tract, for 5800 MHz.

The visualization depicted in Figure 16 offers insights into the spatial distribution of SAR within the HUGO model. It showcases how the electromagnetic energy is absorbed and distributed throughout the simulated human body at the specified frequency. This information is valuable for assessing potential health risks associated with electromagnetic exposure and ensuring compliance with safety guidelines.

An interesting observation is made regarding the distribution of average Specific Absorption Rate (SAR) on a 10 g mass within the different layers of the hand wrist. It is noted that the SAR decreases slightly from the skin layer to the adipose layer. Subsequently, a sharp decrease in SAR is observed at the muscle layer, followed by a further reduction near the bone.

Furthermore, the study finds that the average SAR values at the center of the top of the wrist are

higher than the edges. This discrepancy can be attributed to the positioning of the antenna at the center of the wrist. Importantly, the SAR values obtained for each layer of the hand wrist satisfy the SAR requirements set by the FCC (Federal Communications Commission) standards. The FCC standard specifies a SAR limit of 4 W/kg for the body excluding the head [19, 20]. Based on the obtained results, it is concluded that the WCE antenna exhibits SAR values that are below the FCC-defined limit. The maximum SAR value recorded is 3.05 W/kg, which occurs at the 5800 MHz frequency. These findings underscore the compliance of the WCE antenna with the safety guidelines outlined by the FCC, ensuring that the antenna's SAR values remain within acceptable limits and pose no significant risk to human health.

4. CONCLUSION

This paper attempts to cover common known problems with wireless capsule endoscopy and the research that has been done to solve them. Starting with the transmission part, we have discussed several basic standards of the WEC antenna for operation in/on the human body. The signal transmission efficiency of the antenna will directly decide the quality of the actual images received and the rate of power consumption. The two basic types of transmitting antenna are spiral antennas and conformal antennas. We have observed recent proposals of path loss models aimed at enhancing WCE data transmission from inside to outside the human body. However, only a limited number of studies have explored the development of optimized antennas to further improve this transmission.

Our future work and contributions may focus on real-time WCE localization based on beamforming and localization techniques taking into account adequate path loss models of internal to external communication and optimized antennas. To this end, our position is that first of all the trade-off between transmission quality and hardware must be optimized with regard to cost and efficiency, and the WEC must be designed with a loss of realistic path and optimized antenna. This optimization will make the localization algorithm more efficient and more reliable.

ACKNOWLEDGMENT

The authors would like to thanks the University Imam Mohammad Ibn Saud Islamic (IMSIU) for their funding under the project RG-21-09-47.

REFERENCES

1. Basar, M. R., F. Malek, K. M. Juni, M. Shaharom Idris, and M. I. M. Saleh, "Ingestible wireless capsule technology: A review of development and future indication," *International Journal of Antennas and Propagation*, Pt. 6, 1807165.1–1807165.14, 2012, doi: 10.1155/2012/807165.
2. Lim, E., C. W. Jing, W. Zhao, G. Juans, and M. Zhang, "Wireless capsule antennas," *Lecture Notes in Engineering and Computer Science*, Vol. 2203, 726–729, 2013.
3. Latif, S. I., D. F. Tapia, D. R. Herrera, and M. S. Nepote, "A directional antenna in a matching liquid for microwave radar imaging," *International Journal of Antennas and Propagation*, Pt. 5, 751739.1–751739.8, 2015, doi: 10.1155/2015/751739.
4. Seo, D.-W., J.-H. Lee, and H. Lee, "Integration of resonant coil for wireless power transfer and implantable antenna for signal transfer," *International Journal of Antennas and Propagation*, Pt. 2, 7101207.1–7101207.7, 2016, doi: 10.1155/2016/7101207.
5. Miah, Md. S., A. N. Khan, C. Icheln, K. Haneda, and K.-I. Takizawa, "Antenna systems for wireless capsule endoscope: Design, analysis and experimental validation," *IEEE Transactions on Antennas and Propagation*, 2017, doi: 10.1109/TAP.2017.2705023.
6. Shadid, R. and S. Noghanian, "A literature survey on wireless power transfer for biomedical devices," *International Journal of Antennas and Propagation*, Pt. 1, 4382841.1–4382841.11, 2018, doi: 10.1155/2018/4382841.

7. Kissi, C., M. Särestöniemi, T. Kumpuniemi, S. Myllymäki, M. Sonkki, M. N. Srifi, H. Jantunen, and C. Pomalaza-Raez, "Reflector-backed antenna for UWB medical applications with on-body investigations," *International Journal of Antennas and Propagation*, Pt. 3, 6159176.1–6159176.17, 2019, doi: 10.1155/2019/6159176.
8. Fady, B., A. Tribak, J. Terhzaz, and F. Riouch, "Novel low-cost integrated multiband antenna design customized for smartwatch applications with SAR evaluation," *International Journal of Antennas and Propagation*, Pt. 2, 8833839.1–8833839.14, 2020, doi: 10.1155/2020/8833839.
9. Roman, K. L.-L., G. Vermeeren, A. Thielens, W. Joseph, and L. Martens, "Characterization of path loss and absorption for a wireless radio frequency link between an in-body endoscopy capsule and a receiver outside the body," *EURASIP Journal on Wireless Communications and Networking*, 2014.
10. Tanghe, E., G. Vermeeren, W. Joseph, and L. Martens, "Propagation aspects of a wireless capsule endoscopy link," *EuCAP 2013; European Conference on Antennas and Propagation*, 2013.
11. Agneessens, S., P. van Torre, E. Tanghe, G. Vermeeren, W. Joseph, and H. Rogier, "On-body wearable repeater as a data link relay for in-body wireless implants," *IEEE Antennas and Wireless Propagation Letters*, Vol. 11, 2012.
12. Kurup, D., G. Vermeeren, E. Tanghe, W. Joseph, and L. Martens, "In-to-out body antenna-independent path loss model for multilayered tissues and heterogeneous medium," *Sensors*, Vol. 15, 408–421, 2015.
13. Kurup, D., W. Joseph, E. Tanghe, G. Vermeeren, and L. Martens, "Extraction of antenna gain from path loss model for in-body communication," *Electronics Letters*, Vol. 47, Nov. 10, 2011.
14. Cheng, X., J. Wu, R. Blank, D. E. Senior, and Y. K. Yoon, "An omnidirectional wrappable compact patch antenna for wireless endoscope applications," *IEEE Antennas and Wireless Propagation Letters*, Vol. 11, 1667–1670, 2012.
15. Graepler, F., et al., *Accuracy of the Size Estimation in Wireless Capsule Endoscopy: Calibrating the M2A PillCam*, Elsevier, 2018, doi: 10.1016/j.gie.2007.10.060.
16. Federal Communications Commission, "Specifc absorption rate (SAR) for cellular telephones," 2012. [Online]. Available: https://www.fcc.gov/general/cell-phones-and-specific-absorption-rate.
17. Federal Communications Commission, "Evaluating compliance with FCC guidelines for human exposure to radiofrequency electromagnetic fields," Supplement C edition 01-01 to OET bulletin 65 edition 97-01, Jun. 2001.
18. International commission on non-ionizing radiation protection, "ICNIRP guidelines: For limiting exposure to time-varying electric, magnetic and electromagnetic fields (up to 300 GHz)," *Health Phys.*, Vol. 99, No. 6, 2010.
19. Fady, B., J. Terhzaz, A. Tribak, and F. Riouch, "Integrated miniature multiband antenna designed for WWD and SAR assessment for human exposure," *International Journal of Antennas and Propagation*, 2020, doi: 10.1155/2021/5548834.
20. Wu, T., T. Rappaport, and C. Collins, "The human body and millimeter-wave wireless communication systems: Interactions and implications," *Proc. IEEE Int. Conf. Commun. (ICC)*, 2015.
21. Lawrence, A. J. and G. M. Smith, "Measurement of gastric acid secretion by conductivity," *European Journal of Pharmacology*, Vol. 35, 371–372, 1969.